

Biomolecular implementations of Linear I/O and Feedback Control Systems

Presentation by Tianqi Song

Oishi, Kazuaki, and Eric Klavins. "Biomolecular implementation of linear I/O systems." *Systems Biology, IET* 5.4 (2011): 252-260.

Yordanov, Boyan, et al. "Computational design of nucleic acid feedback control circuits." *ACS synthetic biology* 3.8 (2014): 600-616.

General Goal:

Develop synthetic biochemical systems that can act to automatically control specified variables of a known CRN reaction system.

Papers:

Oishi, Kazuaki, and Eric Klavins. "Biomolecular implementation of linear I/O systems." *Systems Biology, IET* 5.4 (2011): 252-260.

Yordanov, Boyan, et al. "Computational design of nucleic acid feedback control circuits." *ACS synthetic biology* 3.8 (2014): 600-616.

Biomolecular implementation of linear I/O systems

Oishi, Kazuaki, and Eric Klavins. "Biomolecular implementation of linear I/O systems."
Systems Biology, IET 5.4 (2011): 252-260.

I/O System in State Space

$$\dot{\mathbf{x}} = \mathbf{f}(\mathbf{x}, \mathbf{u}) \quad (1)$$

$$\mathbf{y} = \mathbf{g}(\mathbf{x}, \mathbf{u}) \quad (2)$$

where

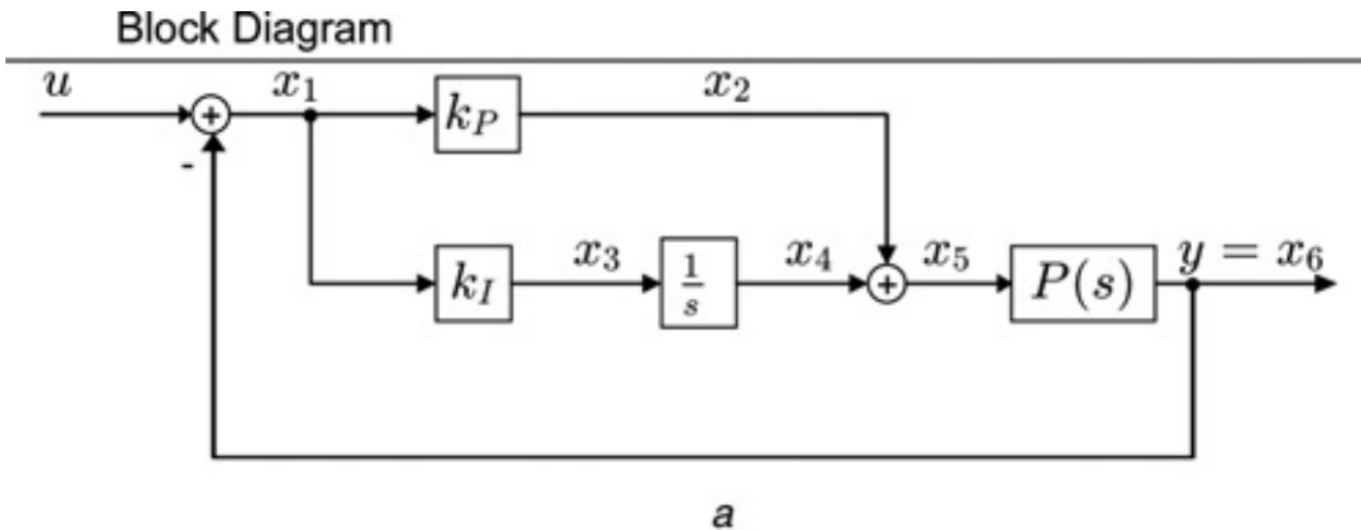
$\mathbf{u}: \mathbb{R} \rightarrow \mathbb{R}^n$ is an input signal,

$\mathbf{y}: \mathbb{R} \rightarrow \mathbb{R}^m$ is an output

$\mathbf{x}: \mathbb{R} \rightarrow \mathbb{R}^p$ is the internal state of the system

$n, m, p \in \mathbb{Z}^+$. Note that signals such as u are functions of time; however, for simplicity we will write u instead of $u(t)$.

Proportional Integral (PI) Controller: Block Diagram



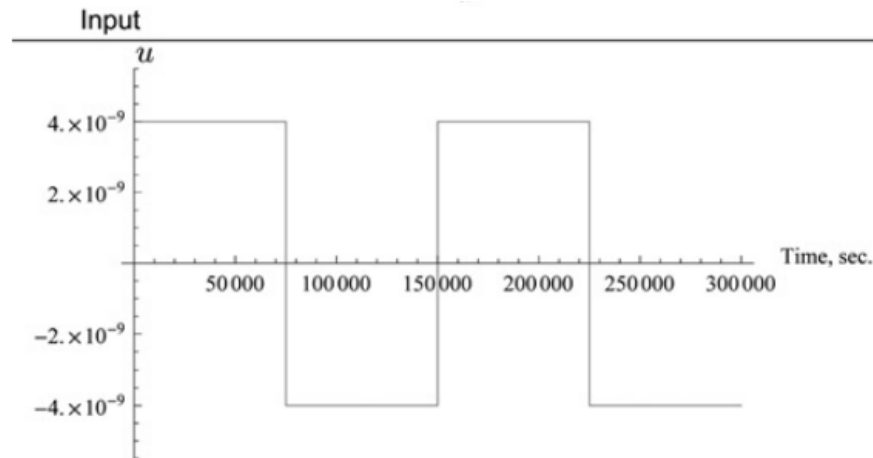
A Block diagram for a PI controller:

- The Proportional Integral (PI) controller is a **feedback system** that tracks an input signal over a class of plants $P(s)$.
- The **plant $P(s)$** is implemented with CRN reactions indicated.

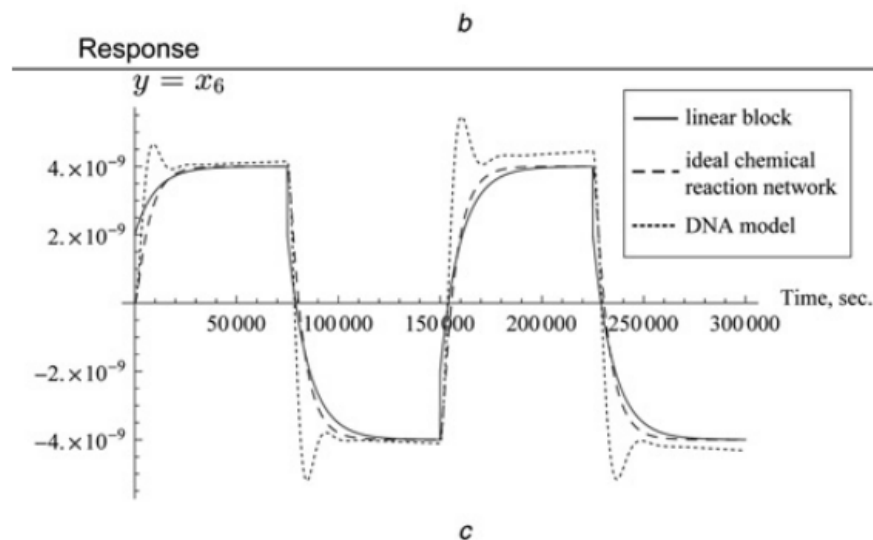
Variables:

- u is input signal
- y is an output signal
- x_1, \dots, x_6 are internal signals
- s is Laplace Transform variable
- $1/s$ is integration in Laplace Transform domain

PI controller block behavior



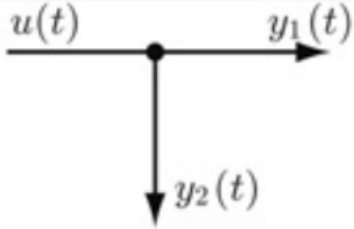
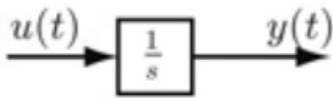
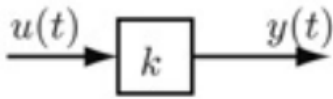
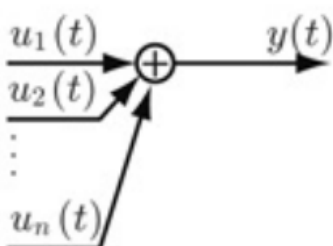
b Input signal driving the PI controller.
The input signal u is a square wave



c. Output trajectories for the ideal PI controller as well as the PI controller implemented with ideal chemical reactions and the DNA model.

- The steady-state error observed in the DNA model of the PI controller is a result of the sequestration of signal molecule $y+$ in intermediate reaction species involved in the left summation block

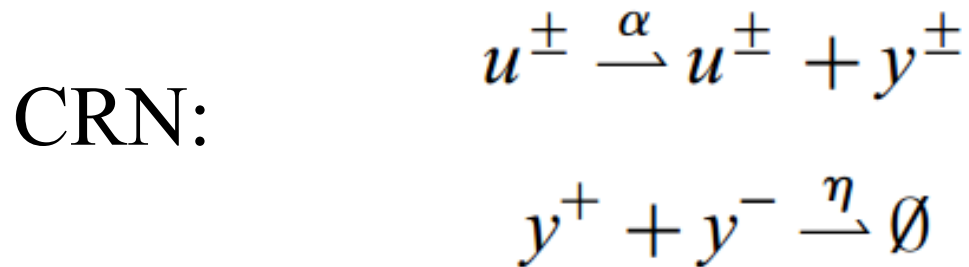
Primitive components of continuous time linear I/O systems

Component Type	Block Diagram	State Space Equations	Transfer Function
Signal Splitting		$\begin{aligned} \dot{x}(t) &= 0 \\ y_1(t) &= u(t) \\ y_2(t) &= u(t) \end{aligned}$	$\frac{Y_i(s)}{U(s)} = 1$
Integration		$\begin{aligned} \dot{x}(t) &= u(t) \\ y(t) &= x(t) \end{aligned}$	$\frac{Y(s)}{U(s)} = \frac{1}{s}$
Gain		$\begin{aligned} \dot{x}(t) &= 0 \\ y(t) &= ku(t) \end{aligned}$	$\frac{Y(s)}{U(s)} = k$
Summation		$\begin{aligned} \dot{x}(t) &= 0 \\ y(t) &= \sum_{i=1}^n u_i(t) \end{aligned}$	$Y(s) = \sum_{i=1}^n U_i(s)$

where $u = u^+ - u^-$

Chemical reaction network for integration

An integration block takes as input a signal $u(t)$ and produces the output signal $y(t) = \int_0^t u(\tau) d\tau + y(0)$ with $t \in \mathbb{R}$. The



**Mass action equations
for CRN of integration:**

$$\dot{u}^{+} = \dot{u}^{-} = 0$$

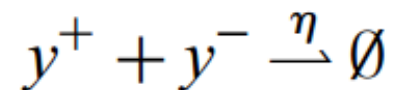
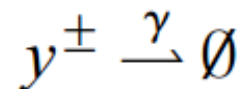
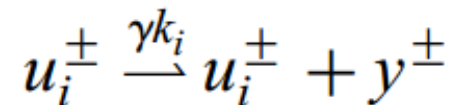
$$\dot{y}^{+} = \alpha u^{+} - \eta y^{+} y^{-}$$

$$\dot{y}^{-} = \alpha u^{-} - \eta y^{+} y^{-}$$

$$\dot{y} = \dot{y}^{+} - \dot{y}^{-} = \alpha u$$

Chemical reaction network for gain and summation

Gain and summation blocks produce output signals that are linear combinations of their inputs. A gain block takes as input a single signal $u(t)$ and produces the output signal $y(t) = ku(t)$ where $k \in \mathbb{R}$. A summation block takes as input the signals $\{u_i(t)\}_{i=1}^n$, and produces the output signal $y(t) = \sum_{i=1}^n u_i(t)$.



Mass action equations for CRN of gain and summation

$$\dot{u}_i^+ = \dot{u}_i^- = 0$$

$$\dot{y}^+ = \gamma \left(\sum_{i=1}^n k_i u_i^+ - y^+ \right) - \eta y^+ y^-$$

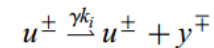
$$\dot{y}^- = \gamma \left(\sum_{i=1}^n k_i u_i^- - y^- \right) - \eta y^+ y^-$$

$$\dot{y} = \gamma \left(\sum_{i=1}^n k_i u_i - y \right)$$

For a constant inputs u_i , the steady state value of y is

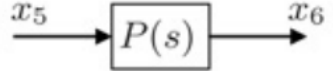
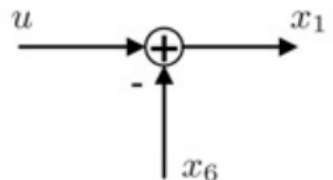

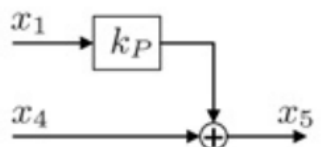
$$\lim_{t \rightarrow \infty} y(t) = \sum_{i=1}^n k_i u_i$$

The chemical representation can be extended to allow negative multiplicative weights. For $k_i < 0$, the catalysis reactions (18) are replaced with



As before, the annihilation reaction drives the concentration of chemical species y^+ and y^- towards a minimal representation of the signal y without affecting the dynamics of the signal y .

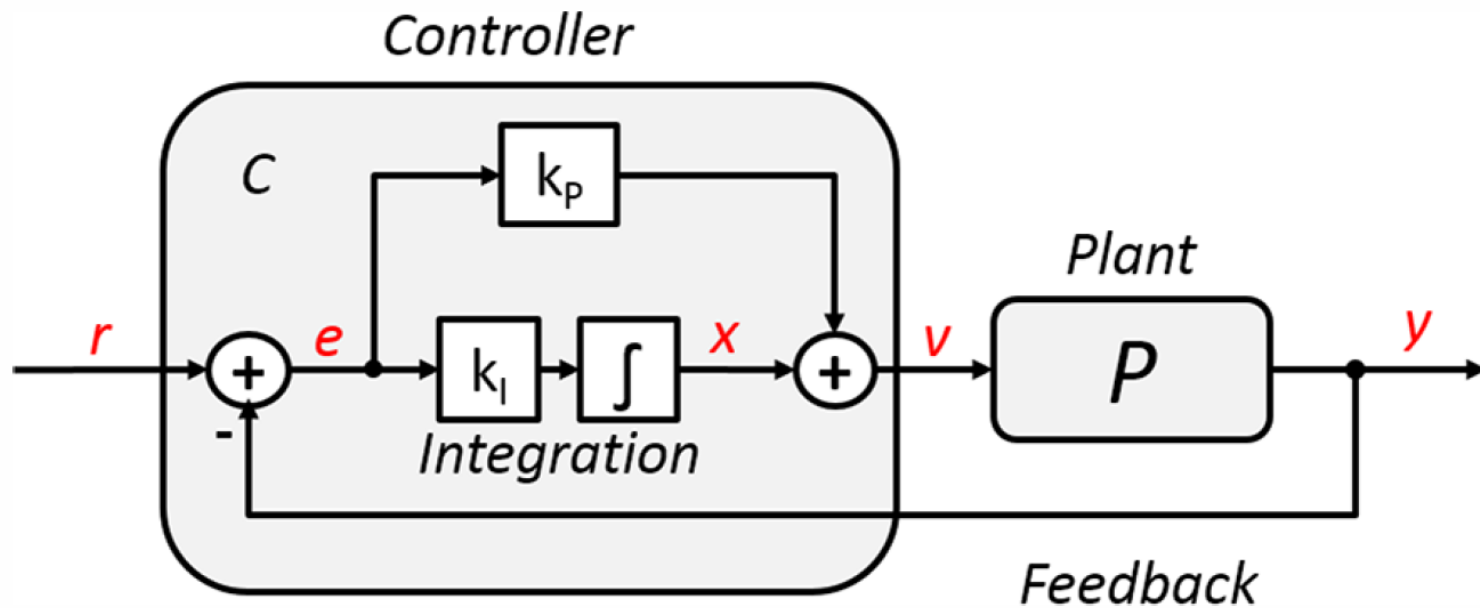
PI controller from implemented in chemical reactions

Component	Ideal Chemical Reactions		
<p>Plant</p> 	\emptyset	$\frac{\gamma^{\delta_{1\lambda}}}{\gamma_{\lambda}}$	x_5^{\pm}
	x_5^{\pm}	$\frac{\gamma^{\delta_{2\lambda}}}{\gamma_{\lambda}}$	\emptyset
	x_6^{\pm}	$=$	x_5^{\pm}
Summation			
	u^{\pm}	$\frac{\gamma_{\lambda}}{\gamma_{\lambda}}$	$u^{\pm} + x_1^{\pm}$
	x_5^{\pm}	$\frac{\gamma_{\lambda}}{\gamma_{\lambda}}$	$x_5^{\pm} + x_1^{\mp}$
	$x_1^+ + x_1^-$	$\frac{\eta_{\lambda}}{\gamma_{\lambda}}$	\emptyset
Weighted Integration			
	x_1^{\pm}	$\frac{k_I \gamma_{\lambda}}{\gamma_{\lambda}}$	$x_1^{\pm} + x_4^{\pm}$
	$x_4^+ + x_4^-$	$\frac{\eta_{\lambda}}{\gamma_{\lambda}}$	\emptyset
Weighted Summation			
	x_1^{\pm}	$\frac{\gamma^{k_P \lambda}}{\gamma_{\lambda}}$	$x_1^{\pm} + x_5^{\pm}$
	x_4^{\pm}	$\frac{\gamma_{\lambda}}{\gamma_{\lambda}}$	$x_4^{\pm} + x_5^{\pm}$
	x_5^{\pm}	$\frac{\gamma_{\lambda}}{\gamma_{\lambda}}$	\emptyset
	$x_5^+ + x_5^-$	$\frac{\eta_{\lambda}}{\gamma_{\lambda}}$	\emptyset

Nucleic Acid Feedback Control Circuits

Yordanov, Boyan, et al. "Computational design of nucleic acid feedback control circuits." *ACS synthetic biology* 3.8 (2014): 600-616.

Feedback control system



Feedback control system composed of a physical plant P and a controller C .

- The **error signal e** is difference between the reference signal r and the plant output y .
- The **controller** automatically computes and adjusts the plant input v to minimize the **error and track the reference signal**, according to the tuning parameters K_p and K_i .

Variety of Feedback Control Biochemical Systems Studied:

Plants implemented using ideal chemical reactions were coupled to a Proportional Integral (PI) controller implemented using for comparison:

(A) DNA strand displacement circuit design:

K Oishi and E Klavins. Biomolecular implementation of linear I/O systems. *IET Systems Biology*, 5(4):252–260, 2011

(B) Enzymic circuit design:

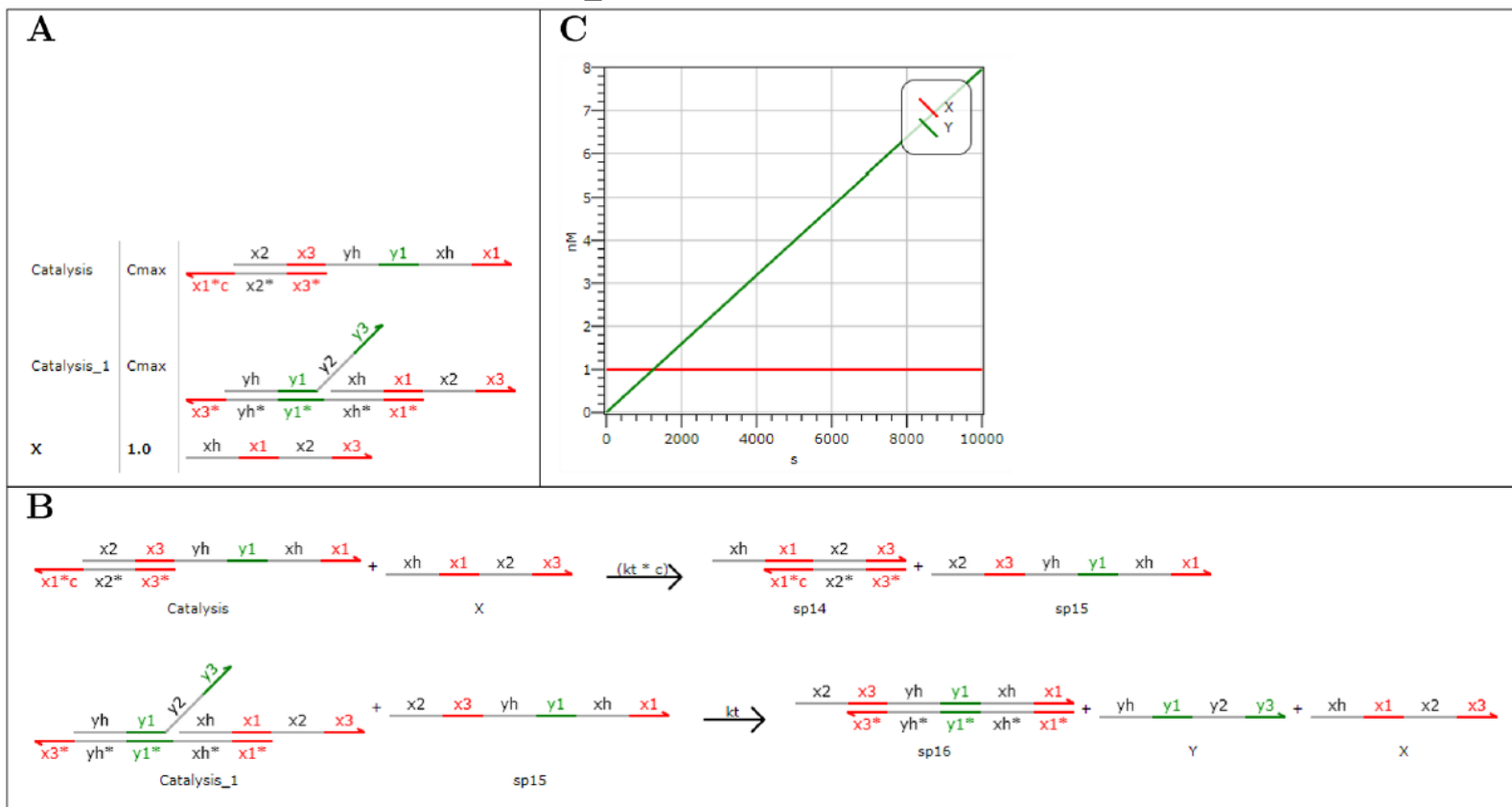
Kevin Montagne, Raphael Plasson, Yasuyuki Sakai, Teruo Fujii, and Yannick Rondelez. Programming an in vitro DNA oscillator using a molecular networking strategy. *Molecular systems biology*, 7(466):466, February 2011

(C) Genelet circuit design:

Jongmin Kim and Erik Winfree. Synthetic in vitro transcriptional oscillators. *Molecular Systems Biology*, 7:465, Feb 2011

Preliminaries: Visual DSD implementation of a catalytic 4-domain DNA strand displacement circuit

The DNA strand displacement circuit design: . K Oishi and E Klavins. Biomolecular implementation of linear I/O systems. IET Systems Biology, 5(4):252–260, 2011



(A) Initial concentrations (nM) of strand X and complexes Catalysis and Catalysis1, with $C_{max} = 1000$ nM.

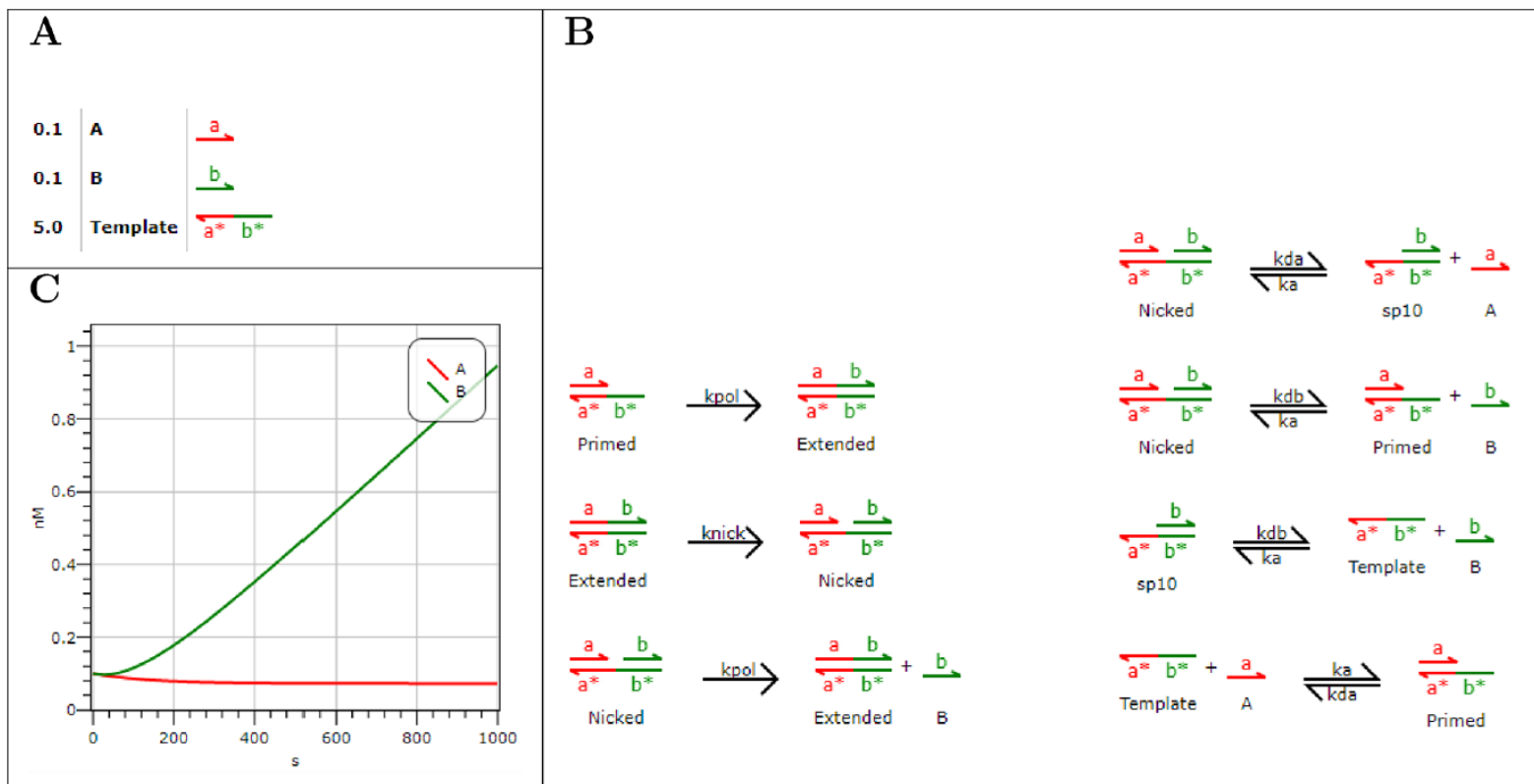
(B) Strand displacement reactions generated automatically from the initial conditions by Visual DSD, with toehold binding rate $k_t = 10^{-3} \text{ nM}^{-1} \text{ s}^{-1}$. The binding rate of toehold x1 is modulated by the degree of complementarity $c = 8 \times 10^{-4}$ resulting in an effective binding rate of $8 \times 10^{-7} \text{ nM}^{-1} \text{ s}^{-1}$.

(C) Corresponding simulation results.

Preliminaries: Visual DSD implementation of a catalytic DNA toolbox circuit

The Enzymic circuit design: Kevin Montagne, Raphael Plasson, Yasuyuki Sakai, Teruo Fujii, and Yannick Rondelez.

Programming an in vitro DNA oscillator using a molecular networking strategy. *Molecular systems biology*, 7(466):466, February 2011



(A) Initial concentrations (nM) of strands A, B, and Template.

(B) Enzymatic reactions modeled explicitly in Visual DSD (left column), with rates $k_{pol} = 0.2833 \text{ s}^{-1}$ and $k_{nick} = 0.05 \text{ s}^{-1}$. Remaining reactions generated automatically from the initial conditions by Visual DSD (right column), with rates $k_a = 4.3333 \times 10^{-4} \text{ nM}^{-1} \text{ s}^{-1}$, $k_{da} = 0.0383 \text{ s}^{-1}$, and $k_{db} = 0.0135 \text{ s}^{-1}$ used as binding and unbinding rates for domains a and b.

(C) Corresponding simulation results.

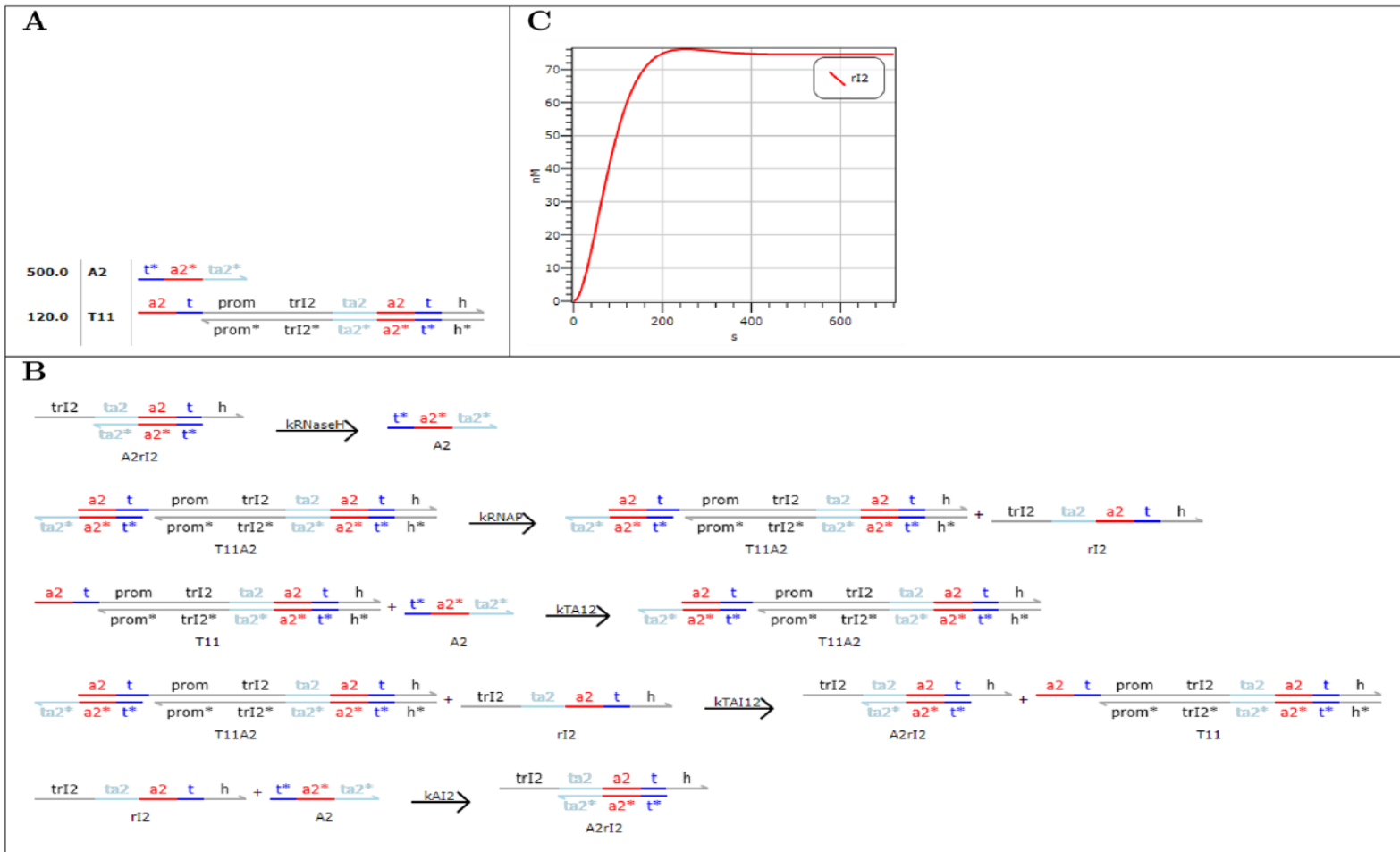
Preliminaries : Visual DSD implementation of a genelet circuit with a negative feedback loop

The Genelet circuit design: Jongmin Kim and Erik Winfree. Synthetic in vitro transcriptional oscillators. *Molecular Systems Biology*, 7:465, Feb 2011 (except that here the output of the genelet directly inhibits its own production)

(A) Initial concentrations (nM) of strand A and genelet T11.

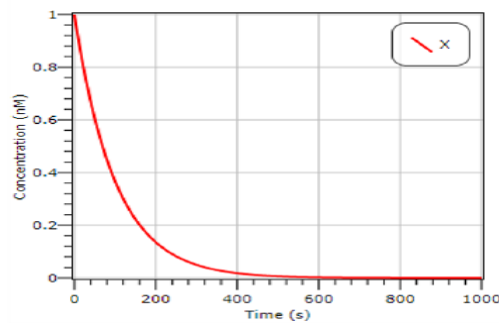
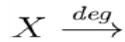
(B) The first two enzymatic reactions were modeled explicitly in Visual DSD, with rates $k_{RNAP} = 0.0323 \text{ s}^{-1}$ and $k_{RNaseH} = 0.0196 \text{ s}^{-1}$. The remaining reactions were generated automatically from the initial conditions by Visual DSD, with rates $k_{TA12} = 1.4 \times 10^{-5} \text{ nM}^{-1} \text{ s}^{-1}$, $k_{TAI12} = 1.4 \times 10^{-4} \text{ nM}^{-1} \text{ s}^{-1}$ and $k_{AI2} = 3.1 \times 10^{-5} \text{ nM}^{-1} \text{ s}^{-1}$, used as binding rates for composite domain (a₂;t), domain ta₂ and composite domain (ta₂;a₂;t), respectively.

(C) Corresponding simulation results.

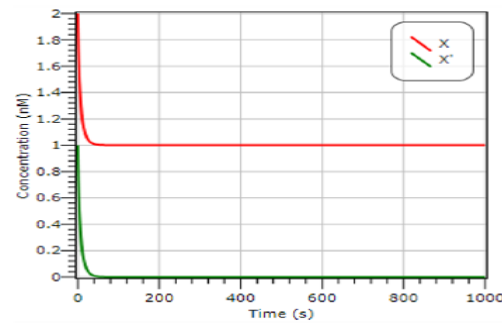
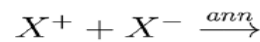


Chemical reaction models and simulations of basic components

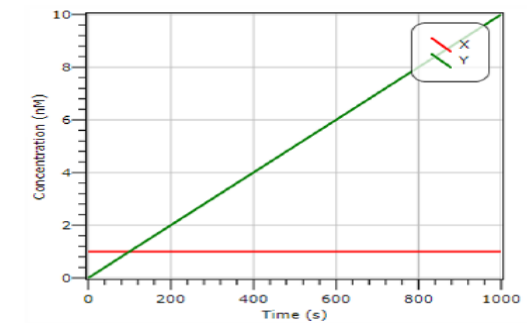
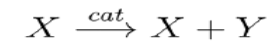
A. Degradation



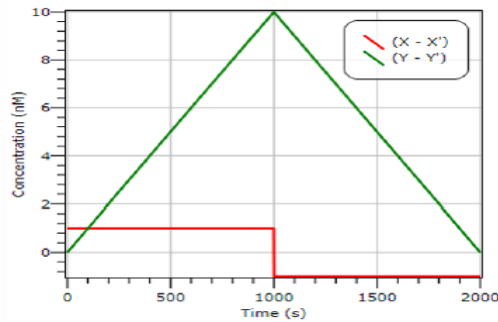
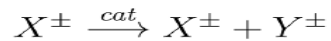
B. Annihilation



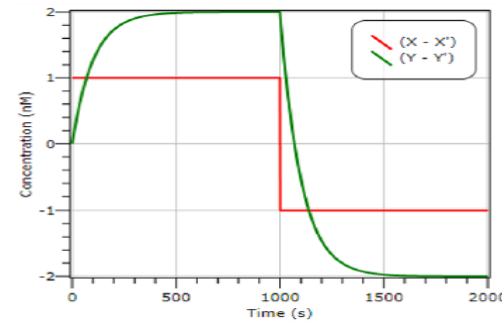
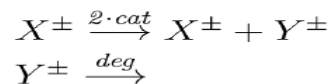
C. Catalysis



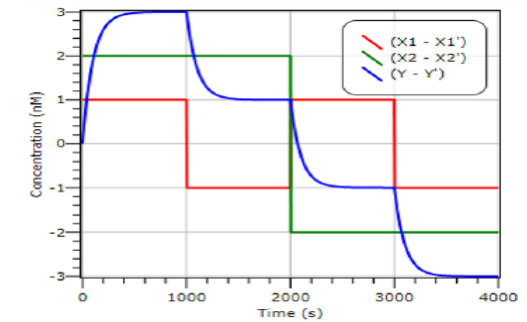
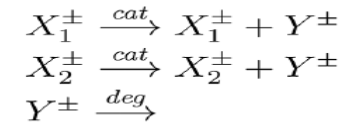
D. Integration



E. Gain

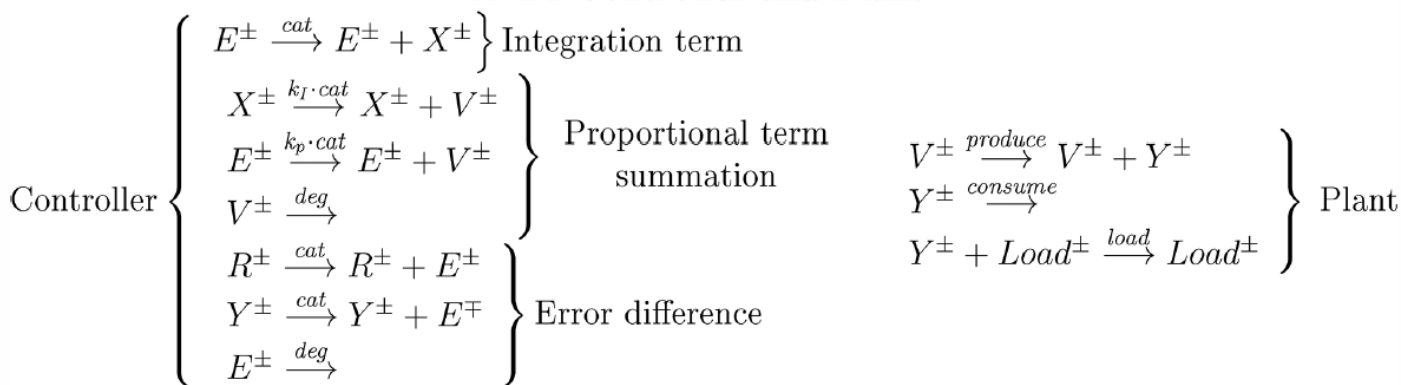


F. Summation

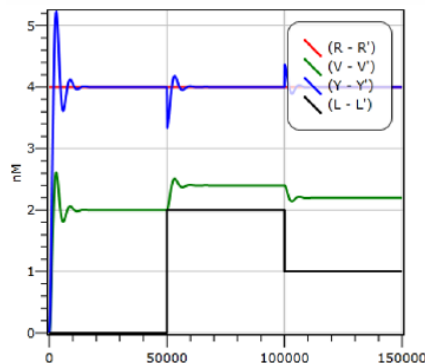


Proportional Integral controller, connected to a production plant

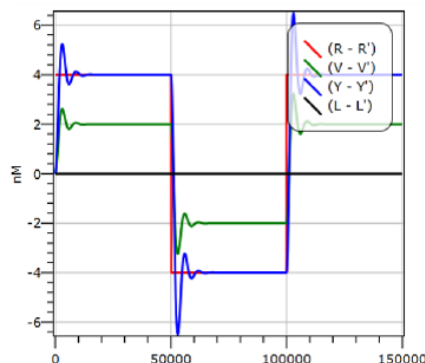
A. PI Controller and Plant



B. PI variable load



C. PI variable reference

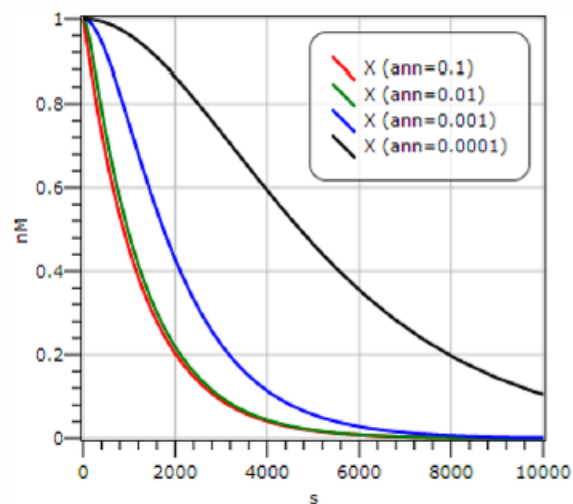


Chemical reaction model and simulation of a Proportional Integral controller, connected to a production plant.

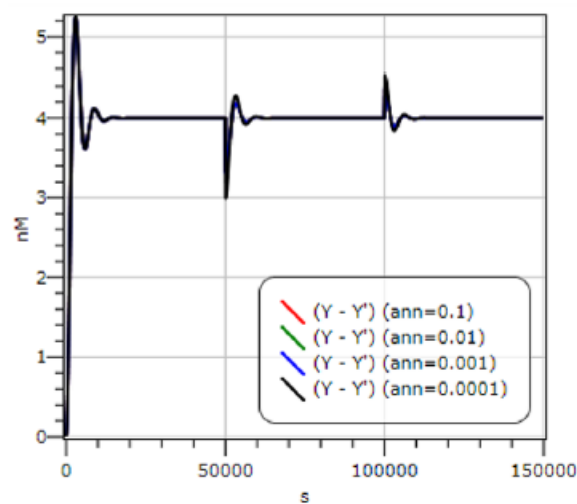
- For each pair of complementary signals X^\pm , Y^\pm , E^\pm , V^\pm , and R^\pm an annihilation reaction is also present, for example $X^+ + X^- \rightarrow \text{Ann } \emptyset$ for signals X^\pm , but is omitted for conciseness.
- Simulations were run for controller tuning parameters $k_I = k_p = 1.0$ and reaction rates $\text{deg} = \text{cat} = 0.0008 \text{ s}^{-1}$, $\text{ann} = 0.01 \text{ nM}^{-1} \text{ s}^{-1}$, $\text{produce} = 0.2 \text{ s}^{-1}$, $\text{consume} = 0.1 \text{ s}^{-1}$, and $\text{load} = 0.01 \text{ nM}^{-1} \text{ s}^{-1}$.
- Plots show absolute values of reference R , plant input V , plant output Y , and load L .

Using a simplified catalytic degradation scheme

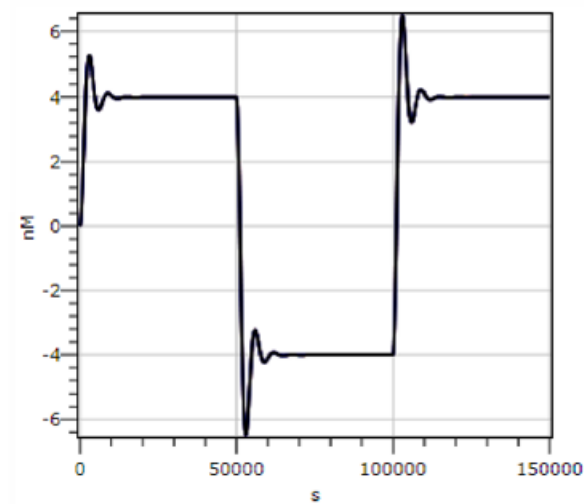
A. Catalytic degradation



B. PI variable load



C. PI variable reference



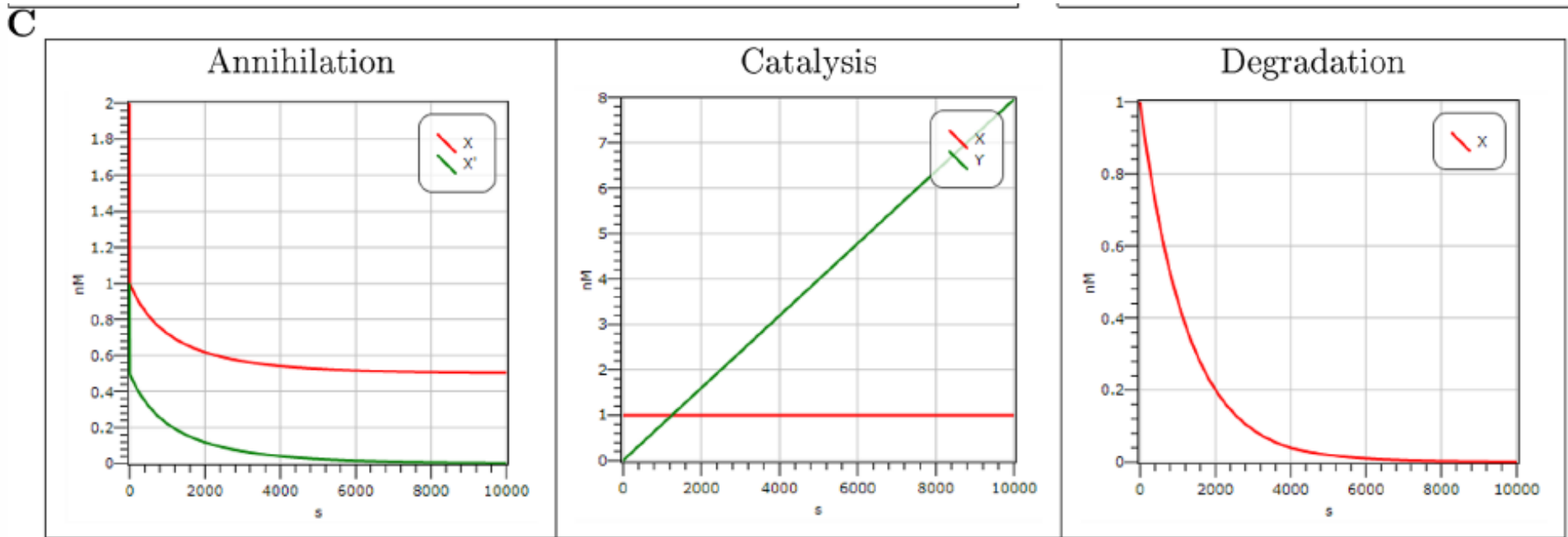
Simulation results for a simplified catalytic degradation scheme in which each degradation reaction $X_{\pm} \xrightarrow{\text{deg } \emptyset}$ is replaced by a catalytic reaction $X_{\pm} \xrightarrow{\text{deg } X_{\pm} + X_{\mp}}$ together with an annihilation reaction $X_{\pm} + X_{\mp} \xrightarrow{\text{ann } \emptyset}$.

In each case, standard degradation was compared with catalytic degradation for $\text{deg} = 0.0008 \text{ s}^{-1}$ and $\text{ann} \in \{0.1, 0.01, 0.001, 0.0001\}$; $\text{nM}^{-1} \text{ s}^{-1}$.

(A) For fast annihilation reactions, catalytic degradation accurately approximates standard degradation, with $\text{ann} = 0.1$ indistinguishable from standard degradation (not shown). However, the approximation breaks down as we approach $\text{ann} \approx \text{deg}$.

(B–C) Nevertheless, the correct behavior of the PI controller is still achieved using the catalytic degradation approximation.

Simulation of two-domain strand displacement implementation of annihilation, catalysis, and degradation reactions



(C) Simulation results for each implementation. Rate constants $k_u = k_t = 0.001 \text{ nM}^{-1} \text{ s}^{-1}$ and constant $c = 0.0008$ were used for all simulations.

Yordanov, Boyan, et al. "Computational design of nucleic acid feedback control circuits." *ACS synthetic biology* 3.8 (2014): 600-616.

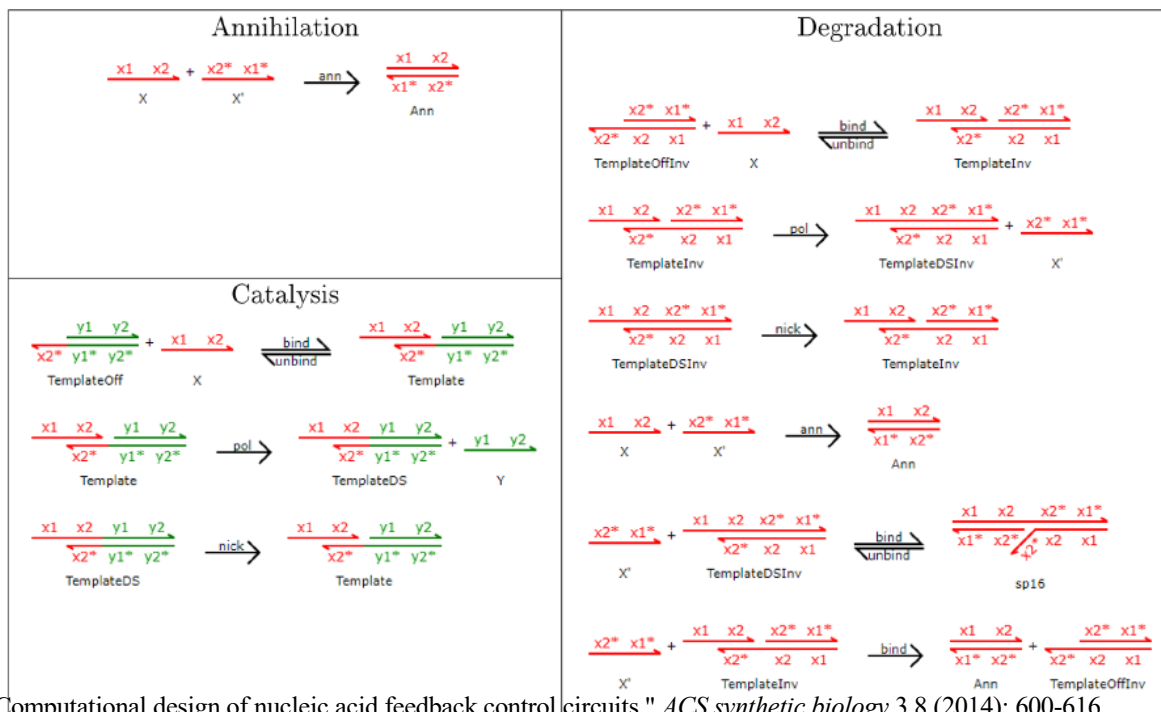
DNA enzyme implementations of the high-level reactions for annihilation, catalysis, and degradation

A

Annihilation		Catalysis		Degradation	
2.0	X	C _{max}	TemplateOff	C _{max}	TemplateOffInv
1.0	X'	1.0	X	1.0	X

(A) Initial concentrations and names for each species, with concentrations expressed in nM.

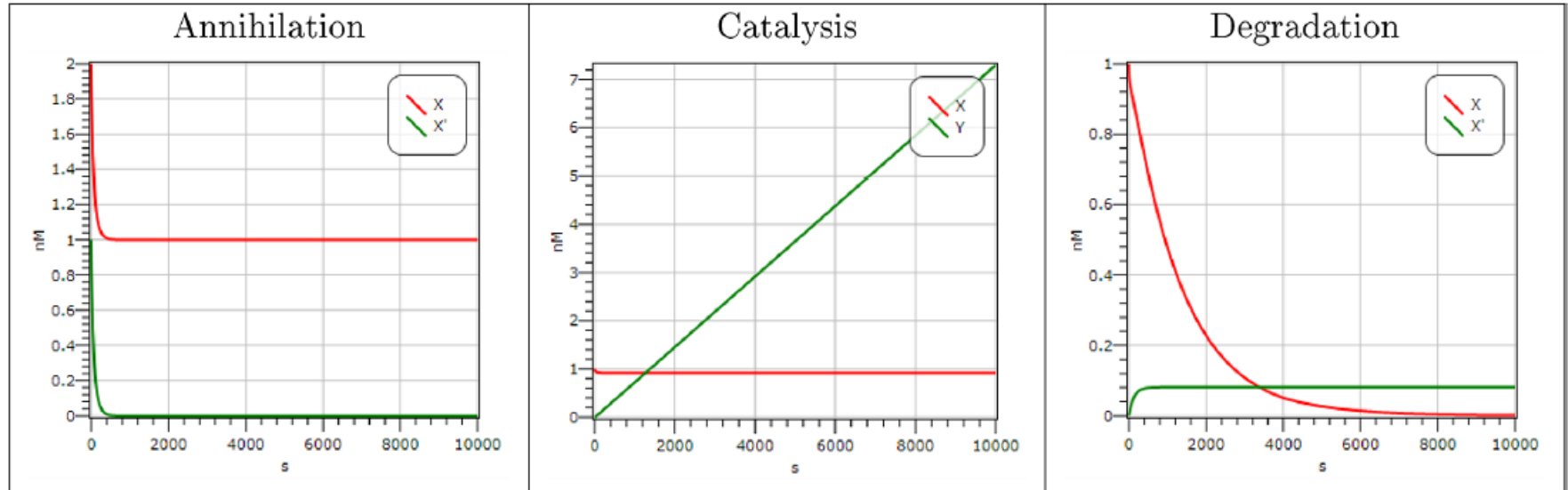
B



B) Low-level reactions for each implementation.
 It is assumed that polymerase and nicking enzymes are in excess with approximately constant concentrations, such that rate constants are first order with $\text{pol} = \text{nick} = 1 \text{ min}^{-1}$

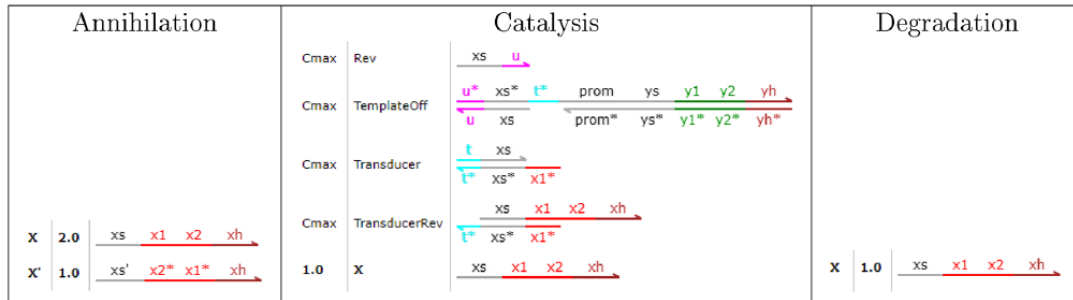
Simulation of DNA enzyme implementations of the high-level reactions for annihilation, catalysis, and degradation

C



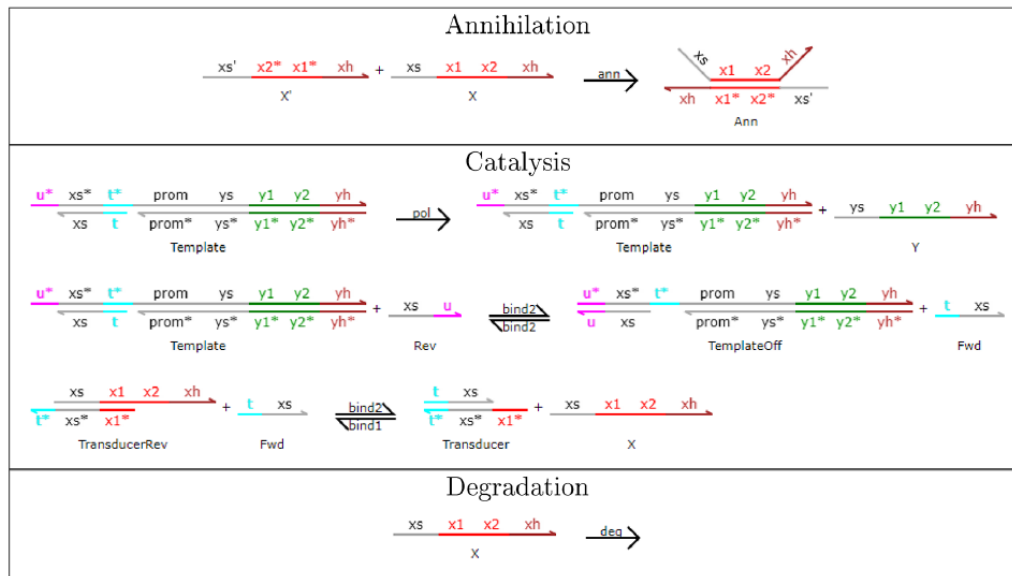
RNA Enzyme implementations of the high-level reactions for annihilation, catalysis, and degradation

A



(A) Initial concentrations and names for each species, with concentrations expressed in nM.

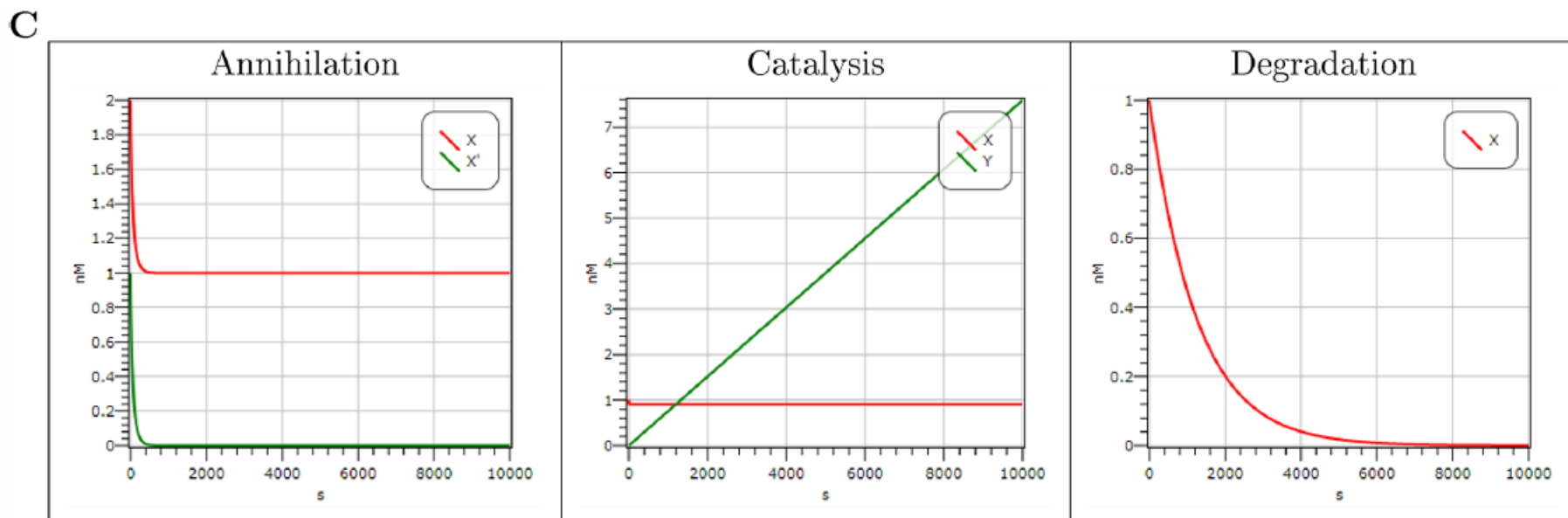
B



(B) Low-level reactions for each implementation.

We assume that polymerase enzymes are in excess with approximately constant concentrations, such that rate constants are first order with $pol = 1 \text{ min}^{-1}$. Similarly, we assume that degradation is first order but that the concentration of enzyme is adjusted for a rate constant of $deg = 0.0008 \text{ s}^{-1.37}$

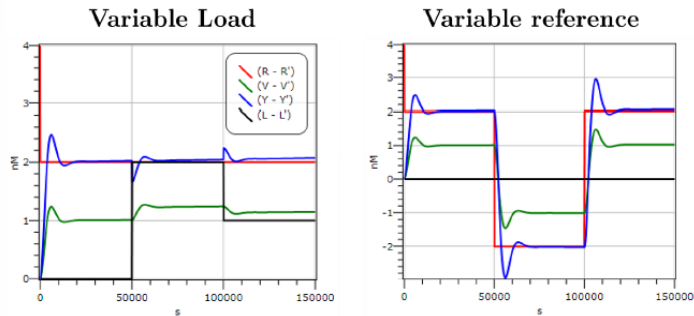
Simulation of RNA Enzyme implementations of the high-level reactions for annihilation, catalysis, and degradation



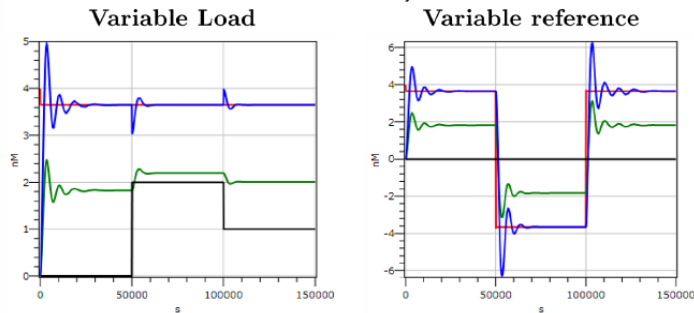
(C) Simulation results for each implementation. Rate constants $\text{ann} = 0.01 \text{ nM}^{-1} \text{ s}^{-1}$, $\text{bind1} = 0.001 \text{ nM}^{-1} \text{ s}^{-1}$, $\text{bind2} = 0.00005 \text{ nM}^{-1} \text{ s}^{-1}$, $\text{unbind} = 0.1126 \text{ s}^{-1}$, and initial conditions $C_{\text{max}} = 1000 \text{ nM}$ were used for all simulations.

Comparison of PI controller designs

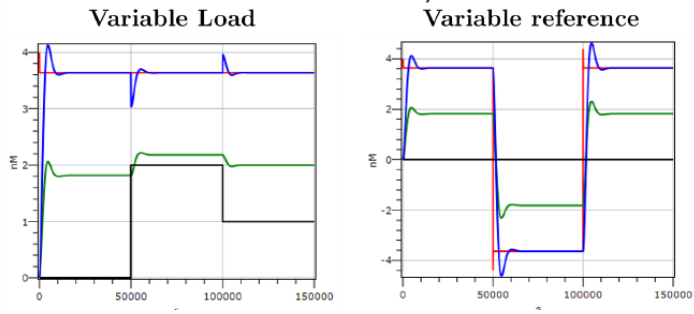
A. Two-domain DSD



B. DNA enzyme



C. RNA enzyme



For all mechanisms, a plant implemented using ideal chemical reactions was coupled to a PI controller implemented using (A) DNA strand displacement, (B) DNA enzyme, and (C) RNA enzyme approaches.

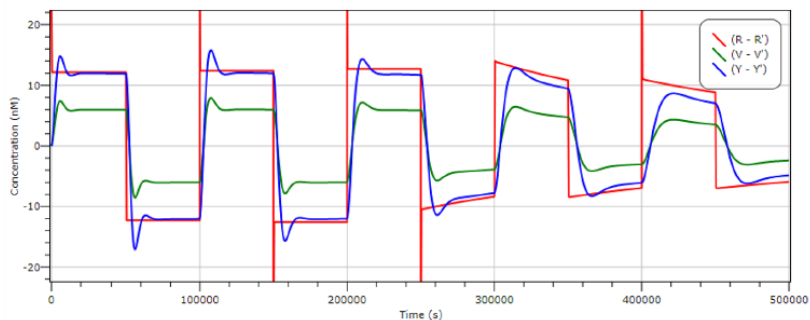
Color Coding:

The difference between the concentrations of positive and negative species are plotted for reference (red), controller output/plant input (green), plant output (blue), and load (black) signals.

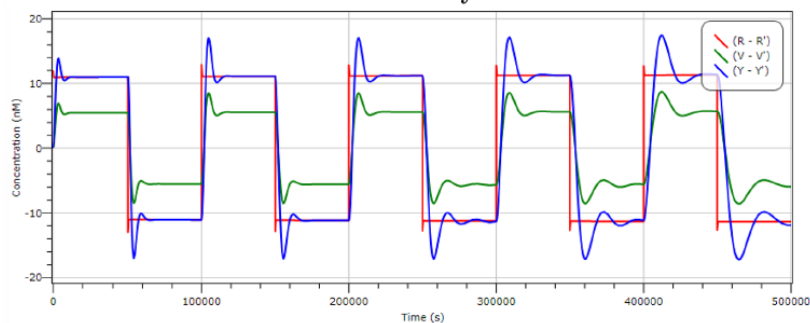
Simulation events were used to trigger the changes in the reference signal and load at predefined times.

Long-term performance of PI controllers

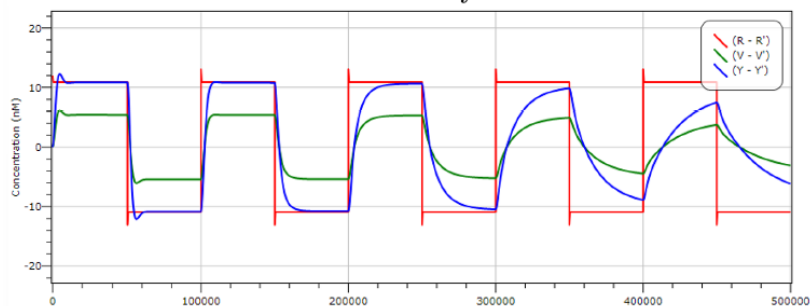
A. Two-domain DSD



B. DNA enzyme



C. RNA enzyme



A plant implemented using ideal chemical reactions:

(A) DNA strand displacement,

(B) DNA enzyme and

(C) RNA enzyme approaches,

An initial pool of 10.0 μM dNTPs (or NTPs) which are consumed through polymerase extension reactions were introduced in the DNA and RNA enzyme implementation designs to account for the consumption of resources.

Color Coding:

The difference between the concentrations of positive and negative species are plotted for the

- **reference (red),**
- **controller output/plant input (green) and**
- **plant output (blue) signals.**

Simulation events were used to trigger the changes in the reference signal at predefined times. For the RNA enzyme design, the plant output drifts away from the reference signal. This takes longer to converge for the DNA enzyme design as resources are consumed, while for the DNA strand displacement design the reference signal could not be accurately modulated over the course of the experiment.

Comparisons and Future Challenges

	Advantages	Challenges
DNA strand displacement	<ul style="list-style-type: none"> *DNA signals can consist of multiple domains and can be relatively long, thus reducing interference between signals. *Toehold-mediated strand displacement can be used to limit interference between components, allowing systems to scale to large numbers of molecular species and reactions. *Catalytic reactions consume the catalyst and quickly produce both catalyst and product, limiting retroactivity between components. *No additional enzymes are required: the entire system can be constructed from DNA. 	<ul style="list-style-type: none"> *Energy is obtained by converting active strands and gates to inert waste, meaning that strands and gates need to be continually supplied for computation to be sustained over long periods. This is potentially challenging to do in a cellular context. *The lack of enzymes for degradation or production of strands means that all computations need to be implemented as strand displacement reactions. This increases the number of components that are needed. *Annihilation rates are limited by the rates of toehold mediated strand displacement, which are generally slower than rates of DNA hybridization.
DNA enzymes	<ul style="list-style-type: none"> *Most reactions are implemented by enzymes which operate with very high efficiency. *The use of multiple categories of enzymes means that complex systems can be designed with only a small number of strands. *The dynamic behavior of systems is relatively well understood 	<ul style="list-style-type: none"> *Additional enzymes need to be provided for the system to function. *Signals are represented as single strands, which need to be relatively short so that they can bind reversibly to a template. As the number of species increases, this could potentially result in cross-talk between species. *Nicking enzymes place additional sequence constraints on signals. *Bimolecular interactions are not directly expressible and need to be encoded in terms of catalysis and inhibition. Alternatively, custom solutions can be tailored to a particular system design, such as mechanisms for strand annihilation. *Enzymes such as polymerase and exonuclease are not sequence specific, which constrains system design.
RNA enzymes	<ul style="list-style-type: none"> *The use of transcriptional machinery and enzymes means that computations can be designed with relatively small numbers of strands. *The use of RNA enables more flexibility in the design, such as using enzymes that enable sequence-specific degradation of RNA. *DNA signals can consist of multiple domains and can be relatively long, resulting in reduced signal interference. *Hybrid designs involving strand displacement, transcriptional regulation and enzymatic processing can be combined. This gives a high degree of design flexibility. 	<ul style="list-style-type: none"> *Additional transcriptional machinery needs to be provided, which complicates the experimental setup. *The additional complexity means that potential sources of interference are less well-understood. *Bimolecular interactions are not directly expressible and custom mechanisms for strand annihilation are required.